Electronic Supplementary Material (ESI) for Analyst.
This journal is © The Royal Society of Chemistry 2023

Supplementary Information

Analysis of the volatile monoterpene composition of citrus essential oils by photoelectron spectroscopy employing continuously monitored dynamic headspace sampling

Hassan Ganjitabar [a)] [c)], Rim Hadidi [b)] [d)], Gustavo A. Garcia [b)], Laurent Nahon [b)], Ivan Powis [a)] *

[a] School of Chemistry, The University of Nottingham, University Park, Nottingham NG7 2RD, UK

[b)] Synchrotron SOLEIL, l'Orme des Merisiers, Saint Aubin BP 48, 91192 Gif sur Yvette Cedex, France.

[c)] Current address : School of Mathematics, Statistics and Physics, Newcastle University, Newcastle upon Tyne, NE1 7RU, UK.

[d)] Current address : Department of Chemistry, University of The Pacific, Stockton, CA 95211, USA

*Corresponding Author:

Email: ivan.powis@nottingham.ac.uk

Phone: +44 115 9513467

Contents

1. Experimental Details

Spectra were recorded with the DELICIOUS 3 double imaging (i^{2}PEPICO) spectrometer [1] mounted in the SAPHIRS [2] doubly skimmed molecular beam chamber permanently attached to the DESIRS undulator-based variable-polarization vacuum ultraviolet (VUV) beamline[3] at Synchrotron SOLEIL. This provides velocity map imaging (VMI) of the electrons, and simultaneous time-of-flight mass determination of coincident ions. The individual electron-ion pair temporal correlation makes it possible to accept only electrons associated with specific ion masses and thus generate mass-tagged photoelectron images and, ultimately, mass-tagged photoelectron spectra.

Photoelectron spectra were recorded by scanning the photon energy while recording photoelectron images. Spatial selection of electrons from the central region of each image is used to filter out near threshold (zero energy) electrons and the variation of this yield with photon energy generates a threshold photoelectron spectrum (TPES). The variant of this approach, slow photoelectron spectroscopy (SPES), [4,5] used for the present study is described further below.

In the present experiments the photon energy was scanned between 7.8 and 10.5 eV with 5 meV steps (typical scan rates of 200 minutes per eV) while recording VMI electron images and coincident ion masses. The monochromator was set to provide energy resolutions in the 4 to 6 meV range. A gas filter in the beamline, filled with Kr, ensured spectral purity by cutting off the higher harmonics from the undulator, [6] while the inadvertent observation of a Kr absorption line ($4p^6 \rightarrow 4p^5[^2P_{3/2}]5s^1$, 10.032 eV) during wavelength scans provided an independent wavelength calibration check.

Beamline settings used to deliver a standard photon flux were carefully controlled and identical sample conditions were used for all measurements. Long term instrumental stability over successive beamtimes was checked by repeating selected measurements on the terpene standards and checking their reproducibility and sensitivity.

2. The slow-photoelectron spectroscopy technique

The slow-photoelectron spectroscopy technique (SPES)[4,5] is used to record high resolution photoelectron spectra. Briefly, 2D VMI electron images were recorded as a function of photon energy and converted to photoelectron spectra, $I(h\nu, eKe)$, using an inverse-Abel transform algorithm.[7] All measurements were normalised against acquisition time and those instrumental settings (slits etc.) that influence the effective delivered photon flux. The coincident ion mass spectra recorded at each photon energy step were used to provide filtering of the electron spectra by the selection of specific masses, or mass ranges, of the accompanying ions.

Threshold photoelectron spectra (TPES) only take into account (near-)threshold electrons with the resolution being roughly equal to the maximum of the accepted electron bandwidth, eKE_{max} : $\mathrm{TPES}(h\nu) = \int_0^{eKE_{max}} I(h\nu, eKE)deKE$. As previously reported,[4,5] the SPES method offers a better compromise between signal and resolution by taking advantage of the energy conservation to increase the electron bandwidth by integrating along the diagonal lines of unity slope $\mathrm{eKE} = \mathrm{h}\nu - IE_i$, where IE_i represents the ionization energy of the i^{th} state. The SPES spectra are then given by the expression: $\mathrm{SPES}(h\nu) = \int_0^{eKE_{max}} I(h\nu + eKE, eKE)deKE$. In the present work the electron bandwidth for the SPES analysis was set as eKE_{max}=100 meV, achieving a calibrated electron energy resolution of 20 meV. Convolving this with the typical photon energy resolution of ~5 meV, provides an estimated overall SPES resolution of better than 21 meV.

As a preparation before the subsequent regression analysis, all spectra were treated with a 7 point cubic Savitzky-Golay low-pass digital filter [8] to remove high frequency noise.

3. Theoretical Model

We assume ideal behaviour for the vapour, so that

$$p_a = x_a P \qquad (1)$$

where p_a is the partial vapour pressure of component *a*, x_a its mole fraction in the vapour and P the total vapour pressure at a given temperature, here 21°C. Intuitively, for a vapour predominantly comprising $C_{10}H_{16}$ terpenes diluted in 0.5 bar He this seems a reasonable approximation.

The ionization rate r_a can be written as

$$r_a = p_a \sigma_a \phi_a \qquad (2)$$

where σ_a is an operational cross-section that includes factors such as geometric factors (ionization region defined by intersection of photon and molecular beams), nozzle backing pressure and the proportionality constant between p_a and number density in the molecular beam, etc. (It can also be assumed to require a 'sensitivity factor' allowing for changes in e.g., alignment between runs at different times.) ϕ_a represents the photon flux during the relevant measurement.

Photoelectron spectra are then given by the product of r and the accumulation/observation time, τ. For the *pure* component a ($x_a = 1$) the *observed* experimental spectrum, S_a, can be written using Eq. (2) as

$$S_a = r_a \tau_a = P \sigma_a \phi_a \tau_a \qquad (3)$$

and S_a^0, the fully normalised spectrum is given as

$$S_a^0 = \frac{S_a}{\phi_a \tau_a} = P \sigma_a \qquad (4)$$

while for a mixture the experimental spectrum will be

$$\begin{aligned} S_{mix} &= \left(\sum_a r_a \right) \cdot \tau_{mix} \\ &= \left(\sum_a p_a \sigma_a \phi_{mix} \right) \cdot \tau_{mix} \\ &= \left(\sum_a x_a P \sigma_a \right) \cdot \phi_{mix} \tau_{mix} \end{aligned} \qquad (5)$$

where in the last step we have used Eq.(1). Then, using Eq. (4) and rearranging we obtain

$$\frac{S_{mix}}{\phi_{mix}\tau_{mix}} = \sum_a x_a S_a^0 \tag{6}$$

Hence, if a complete basis of normalised pure component spectra, S_a^0, is fitted to the normalised spectrum of a mixture, the fitting coefficients, c_a, will equate to the vapour mole fractions, x_a .

Figures

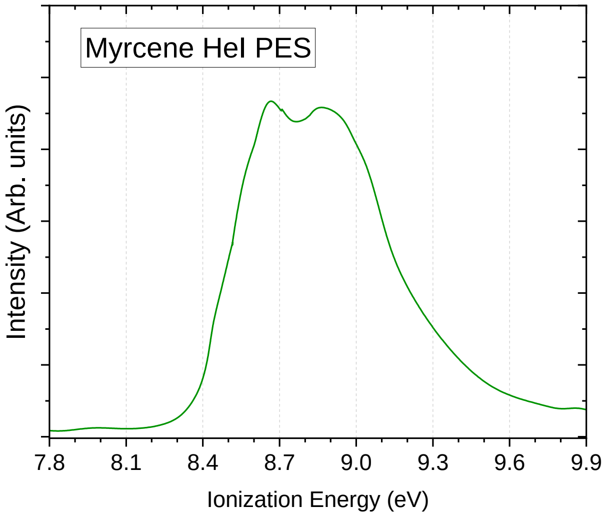

Fig. S1

The HeI photoelectron spectrum of myrcene. Data taken from Ref. [9], Fig. S3.

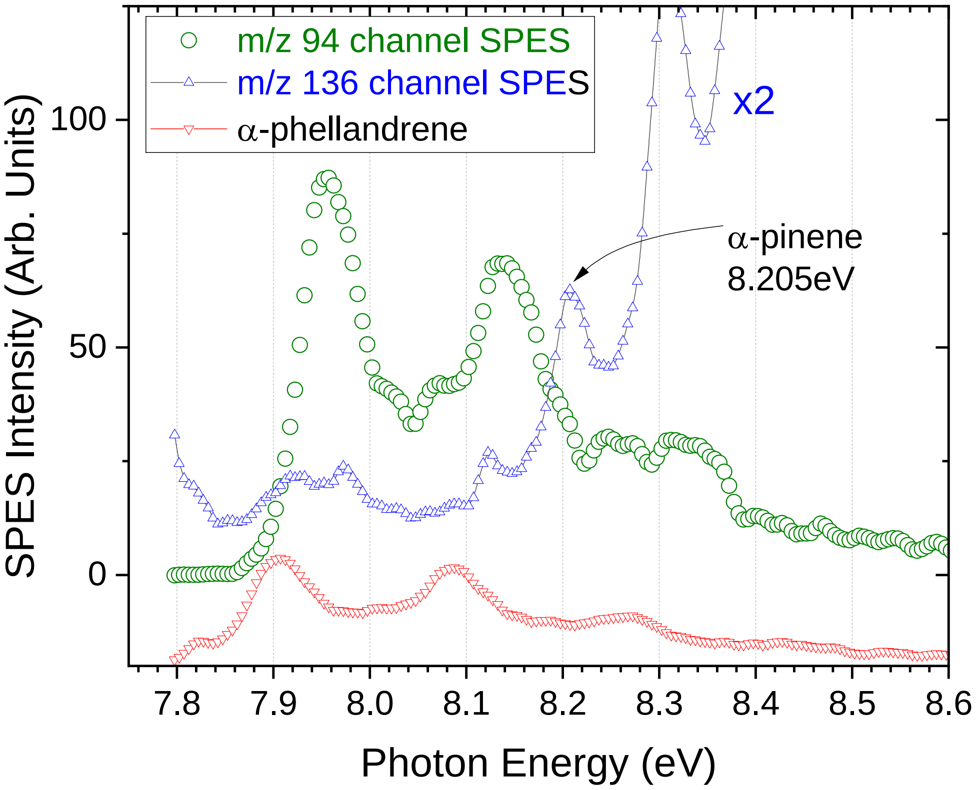

Fig. S2

Low energy regions of the m/z=94 mass filtered lime oil SPES compared to the m/z=136 filtered spectrum. The latter has been plotted with a ×2 vertical scale expansion. The same units for the SPES intensity are used as in Fig. 5 and S5, allowing the relevant intensities of the m/z=94 and m/z=136 features to be judged. Also included is an arbitrarily scaled plot of the α-phellandrene standard in this energy region. The photon energy scales are calibrated to an accuracy of ~10 meV

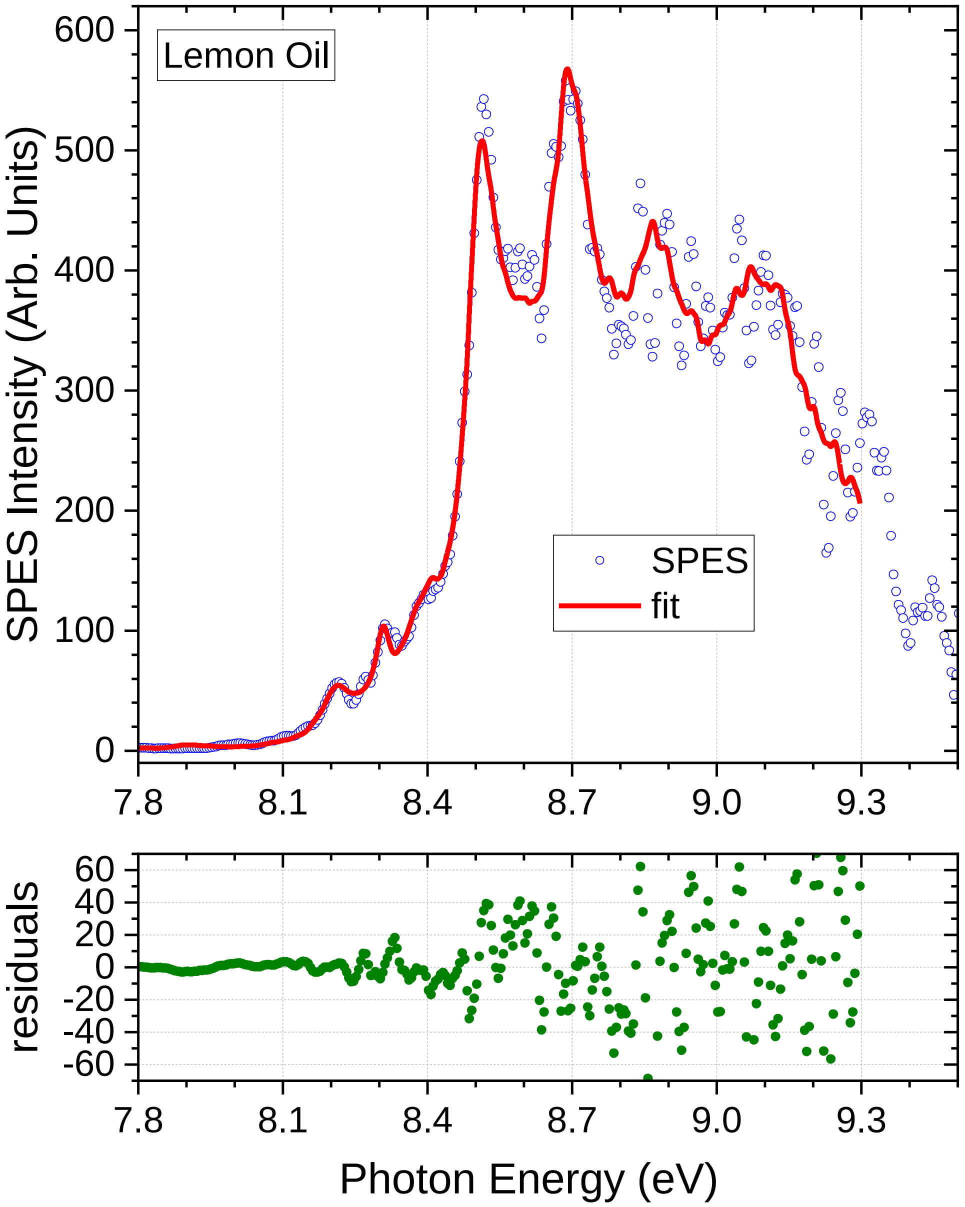

Fig. S3

Non-mass-filtered Californian Lemon oil SPES and the regression fit to the region below 9.3 eV.

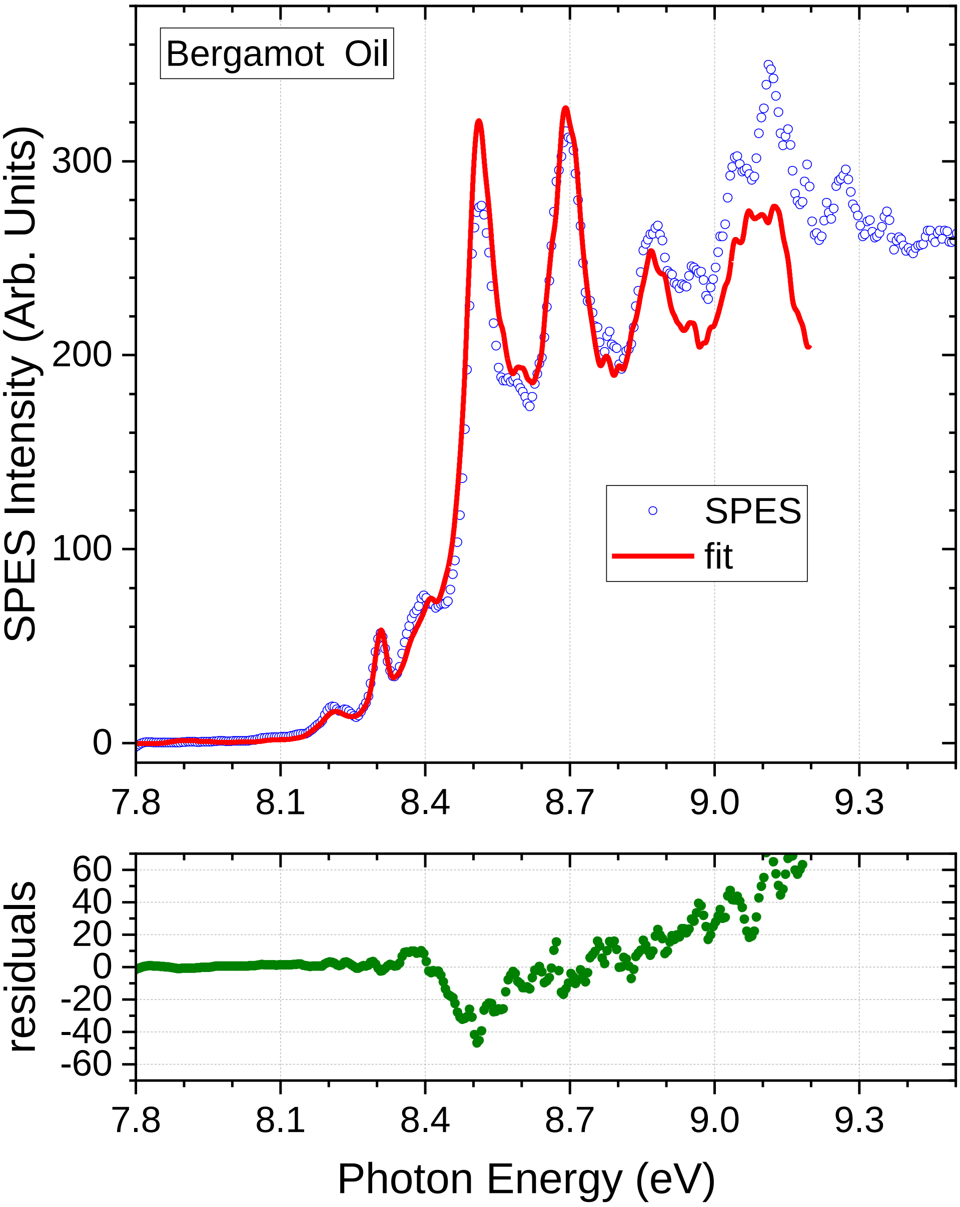

Fig. S4

Non-mass-filtered Bergamot oil SPES and best fit to the region below 9.2 eV.

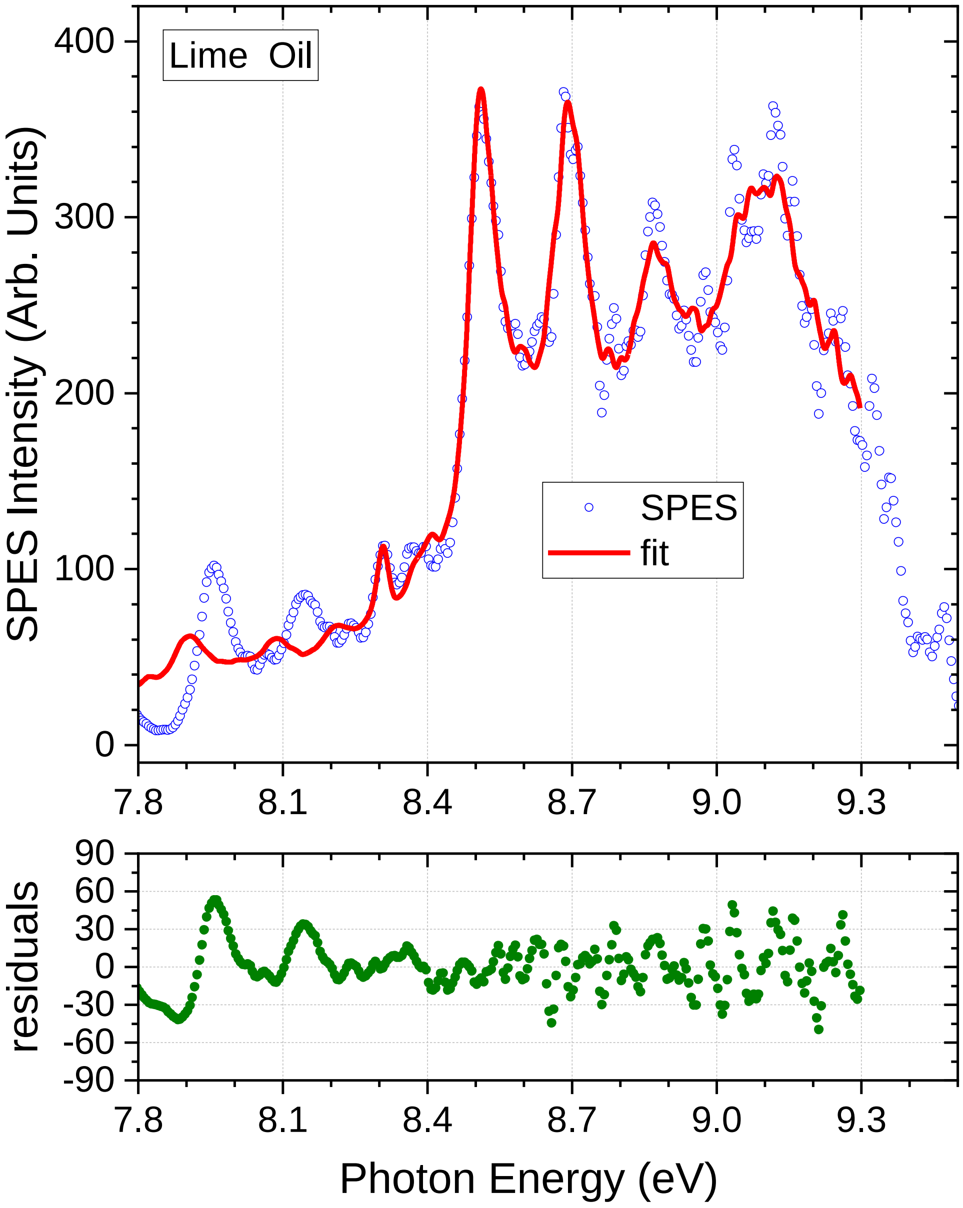

Fig. S5

Non-mass-filtered Lime oil SPES and nonnegative constrained fit to the region below 9.3 eV.

References

References

1. Garcia GA, de Miranda BKC, Tia M, Daly S, Nahon L. DELICIOUS III: A multipurpose double imaging particle coincidence spectrometer for gas phase vacuum ultraviolet photodynamics studies. Review of Scientific Instruments 2013;84(5):053112.
2. Tang XF, Garcia GA, Gil JF, Nahon L. Vacuum upgrade and enhanced performances of the double imaging electron/ion coincidence end-station at the vacuum ultraviolet beamline DESIRS. Review of Scientific Instruments 2015;86(12):123108.
3. Nahon L, Oliveira Nd, Garcia G, Gil JF, Pilette B, Marcouille O, Lagarde B, Polack F. DESIRS: a state-of-the-art VUV beamline featuring high resolution and variable polarization for spectroscopy and dichroism at SOLEIL. Journal of Synchrotron Radiation 2012;19:508-520.
4. Garcia GA, Gans B, Tang X, Ward M, Batut S, Nahon L, Fittschen C, Loison J-C. Threshold photoelectron spectroscopy of the imidogen radical. Journal of Electron Spectroscopy and Related Phenomena 2015;203:25-30.
5. Poully JC, Schermann JP, Nieuwjaer N, Lecomte F, Gregoire G, Desfrancois C, Garcia GA, Nahon L, Nandi D, Poisson L and others. Photoionization of 2-pyridone and 2-hydroxypyridine. Physical Chemistry Chemical Physics 2010;12(14):3566-3572.
6. Mercier B, Compin M, Prevost C, Bellec G, Thissen R, Dutuit O, Nahon L. Experimental and theoretical study of a differentially pumped absorption gas cell used as a low energy-pass filter in the vacuum ultraviolet photon energy range. Journal of Vacuum Science & Technology A-Vacuum Surfaces and Films 2000;18(5):2533-2541.
7. Garcia GA, Nahon L, Powis I. Two-dimensional charged particle image inversion using a polar basis function expansion. Review of Scientific Instruments 2004;75(11):4989-4996.
8. Savitzky A, Golay MJE. Smoothing and Differentiation of Data by Simplified Least Squares Procedures. Analytical Chemistry 1964;36(8):1627-1639.
9. Wang X, Tong S, Ge M, Wang W, Wang D. Photoelectron spectroscopy of terpenoids and prediction of their rate constants in atmospheric oxidation reactions. Chinese Science Bulletin 2010;55(35):4018-4025.